

Structural and Stress Analysis of the Area between Al-Akeider and Mughayer As-Sirhan, Northwestern Badia- Jordan

Abdullah Diabat*

Institute of Earth and Environmental Sciences, Al al-Bayt University, Mafrag, Jordan

Received 29 September, 2014; Accepted 24 May 2015

Abstract

Major tectonic elements of Jordan have been investigated in many studies, in which attention was mainly given to the Dead Sea Transform fault and the associated deformation. However, on a finer scale, our lack of knowledge about the geologic structures as well as the stress regimes of different parts of Jordan is an impediment to understanding the tectonic activities in detail. In this regard, the present study presents the first structural results obtained from fault-slip data, extensional fractures and conjugate shear fractures of the Paleocene- Eocene rock units in northwestern Badia. In aggregate, 142 fault-slip data and 579 fractures were analyzed. Results show that two stress regimes have been distinguished in the study area. The first stress regime is strike-slip which is characterized by σ_1 SHmax oriented NNW-SSE and the second stress regime is extensional (normal faulting) in which σ_1 is vertical, σ_2 (SHmax) and σ_3 (Shmin) is swinging mainly around NE-SW. At least four stress states associated with these regimes were distinguished. The first stress state is characterized by NNW- SSE σ_1 corresponding to the main compression direction in the study area and resulting in the formation of the folds and the related N-S sinistral and WNW-ESE dextral fault sets. The other three states are of extension direction (σ_3); the first is oriented NNE-SSW, and the second is oriented ENE-WSW. These two trends correspond to the main extension defined during the Neogene. The third extension direction is WNW- ESE to E-W which is related to a very late extensional event in Miocene to Pleistocene.

© 2015 Jordan Journal of Earth and Environmental Sciences. All rights reserved

Keywords: Paleostress, Fractures, Tertiary, Northwestern Badia, Jordan.

1. Introduction

Locally derived stress tensors with similar orientations of principal stress axes, together with the values of stress ratio (Sassi and Faure, 1996), distributed over a large region, are considered to represent a regional paleostress solution (Tripathy and Saha, 2013). In deducing lithospheric stresses and their temporal and spatial variation, if any, brittle structures of the earth upper crust are important resources (Angelier, 1989, and 1994). In this regard, structures such as fractures, in general, and faults are used as kinematic indicators to extract useful information about tectonic activities and evolution.

Fracture is, more general, a type of brittle deformation pervasively found in the crust. Depending on their origination and activation mechanism, different fracture modes are identified, such as joints or shear fractures. Pollard and Aydin (1988) defined joints as fractures with evidence of opening mode displacement (i.e., extensional fractures). Others have defined joints as a surface along which there is no appreciable displacement (Price, 1966; Hancock, 1985). Also, shear fractures (e.g., extensional and conjugate) are frequently exposed in association with relatively lower order (major) faults or independently, which can be used in recognizing relative stress regimes.

Faults are one of the most studied fracture types and their relation with their running forces was investigated at various

levels and aspects (Jensen et. al., 2011). The term fault is specifically used to refer to shear fractures, that is, a relatively narrow discontinuity with observable displacement at a given scale (Jensen et. al., 2011). It is accepted that a fault is induced when deviatoric tectonic stresses produce a shear stress that exceeds the shear strength on a particular plane in the rock mass (Kersten, 1990). Consequently, produced kinematic indicators reveal some characteristics of resolved shear stress on a given plane.

Many studies were carried out about the Dead Sea Transform (DST) fault and other related structures to understand the deformation of the region (Fig. 1). In this regard, the regional tectonics of the continental part of the Arabian plate, including Jordan, were studied through macro-structures by many authors (e.g., Quennell, 1958; Burdon, 1959; Bender, 1968, 1974; Mikbel and Zacher, 1981; Quennell, 1983; Mikbel, 1986; Atallah, 1992). Few analyses, however, focused on the regional tectonics based on meso-structures in Jordan (e.g., Salameh and Zacher, 1982; Diabat 1999, 2002, 2009, 2013; Zain Eldeen et. al., 2002; Diabat et. al., 2003, 2004).

Although many details of the tectonic structures of Jordan are now well recognized, these are mainly about the DST fault itself. Other areas in Jordan, except for the DST fault, have received little attention of tectonic and/ or structural studies.

* Corresponding author. e-mail: adiabat@aabu.edu.jo

The area the present study is focused on is one of these poorly investigated areas in Jordan. It represents the northeastern end of the Ibbin-Housha fold belt located few to tens kilometers east of the DST fault, with very obvious brittle structures (e.g., faults, joints, fractures) that deserve to be studied.

The purpose of the present study is to increase our knowledge about the various structures, and to get a better resolution of the paleostresses of the study area on which no such studies are available. This is achieved by analyzing different structural elements, e.g., folds, fractures (joints), and faults in the study area. The field work was carried out with the objectives of determining: (1) structural (e.g., spatial and kinematic) characteristics of fracture sets and (2) determining stress states, where ever possible.

2. Tectonic setting

The study area lies within the east Jordanian Plateau according to Bender (1974). It is located a few kilometers from two major faults; the first is the Jordan Valley Fault (JVF), a sinistral strike-slip fault of the northern segment of the DST fault, and the second is the Sirhan Fault (SF), with extensional characteristics (Fig. 1). The study area is located to the northeastern extremity of Ibbin-Housha fold belt (Figs. 1 and 2). This fold belt is part of the three fold belts in northern Jordan; Halawa-Husn fold belt, Ibbin-Housha fold belt and Balaama-Mafraq fold belt which are located east of (JVF) (Fig. 1). The major trend of these folds is NE to ENE and formed by the compressive stresses related to the northward movement of the Arabian plate and the DST fault (Atallah and Mikbel, 1992).

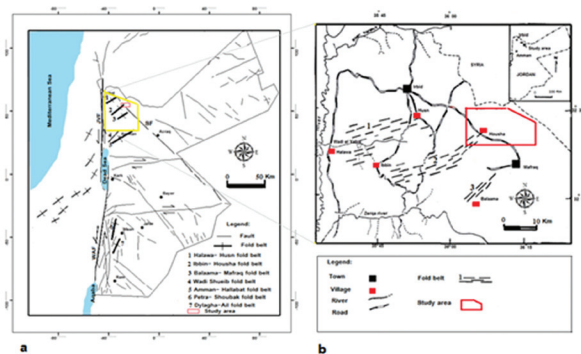


Figure 1. a) Structural pattern of Jordan (compiled from Diabat and Masri, 2005; Atallah and Mikbel, 1992), showing the major structures in Jordan, JVF is Jordan Valley fault, WAF is Wadi Araba fault, SF is Sirhan fault; b) Fold belts in north Jordan (modified after Atallah and Mikbel, 1992).

The DST fault is the most prominent structure in Jordan that resulted from the northward faster movement of the Arabian plate relative to that of the African plate, probably in relation to the Red Sea opening (Quennel, 1958; Garfunkel, 1981). Northward motion of the Arabian plate (Miocene to recent) released opening of the Red Sea and the Gulf of Aden and controls much of the structural pattern of Jordan. This left-lateral transform boundary extends a thousand kilometers from the Gulf of Aqaba in the south to south of Turkey in the north (Freund et al., 1970). In Jordan, the DST fault composed of the Wadi Araba fault (WAF) in the south and the (JVF) in the north (Fig. 1).

3. Stratigraphy

The outcropping rocks in the study area are Upper Cretaceous to Tertiary (Bender, 1974; Powell, 1989) (Fig. 2).

The following represents a brief description of the exposed rocks in the study area; Amman Silicified Limestone Formation (ASL) (Santonian-Campanian) is widespread in Jordan, whereas it crops out only in the southeastern part of the study area. This Formation is of a varying thickness in different locations of Jordan. ASL Formation is distinguished by hard, massive chert beds which form a steep cliff above the pale weathering chalks of Umm Ghudran Formation in central and north Jordan (Powell, 1989). The top of Amman Formation (ASL) is usually distinguished by the first appearance of thick phosphorite beds of Al Hasa Phosphorite Formation (AHP). AHP Formation (late Campanian-early Maastrichtian) consists of a heterogeneous lithology of medium-thick beds of phosphorite, which are intercalated with thin-medium-bedded chert, marl, chalky marl, microcrystalline limestone and oyster-coquina grainstones (Powell, 1989).

The Muwaqqar Chalk- Marl Formation (MCM) (Maastrichtian to Paleocene) is exposed in parts of the study area (Fig. 2). The exposed part is a few meters thick and mainly consists of soft pale yellow, light grey, yellowish to reddish and brown green, occasionally whitish cream chalky marl and marly limestone with calcite in extensional joints. This formation is overlain by Umm Rijam Chert- Limestone Formation (URC) (Eocene), which is widespread and well exposed at the road cuts of the study area. The exposed part of the formation is a few meters thick and consists of limestone, chalky limestone and chert (Fig. 2).

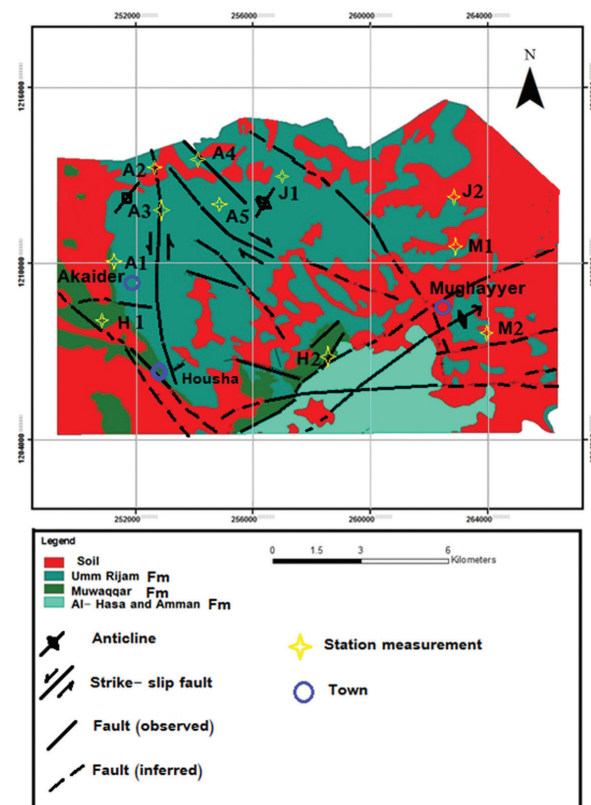


Figure 2. Geological map of the study area with located measurement stations; A1, A2, A3, A4, A5, H1, H2, J1, J2, M1 and M2.

4. Data and method

4.1. Data

Meso-scale brittle structures and statistical analysis methods (Price and Cosgrove, 1990; Hancock, 1991; Twiss and Moores, 1992) were used to infer the fracturing patterns and states of stress controlling the tectonic evolution of the study area.

Determination of paleostress was done using two basic types of brittle structures: (1) faults with slip lines slickensides; (2) fracture planes without slip lines (Angelier 1994; Dunne and Hancock, 1994; Delvaux and Sperner, 2003).

These two types of data were collected from eleven stations along road cuts and abandoned quarries in the study area (Fig. 2). The attitude of fault planes and the associated slickenlines (142 in number), together with the sense of slip, were measured in six stations (i.e., A3, A4, H1, J2, M1 and M2) (Fig. 2 and Table 1). Many exposures were examined, however, only those have been considered as site that have suitable number of faults (at least 7) with associated unquestionable slip sense, as well as significance fractures. Slickenlines and mineral steps were kinematic indicators to determine the sense of slip on the measured faults.

Brittle structures, other than the commonly used slickensides, can also be used as stress indicators (Dunne and Hancock, 1994). The relationship between fractures and principal stress directions implied by the Coulomb fracture

criterion suggests that we can use fractures to estimate the directions of the principal stresses (Price and Cosgrove, 1990; Hancock, 1991; Twiss and Moores, 1992). As this takes place, it is essential to reliably identify the conjugate shear fracture sets that formed or were reactivated at the same time (Lunina et. al., 2005).

Therefore, shear and extensional fractures were measured in the study area particularly, in areas where fault-slip data or marker displacement are not available. The fracture planes (579 in total), which have a significance in the structural analysis, were measured in eight stations (i.e., A1, A2, A3, A4, A5, H1, H2 and J1) and represented as rose diagrams. According to the Coulomb' criteria extensional fractures form parallel to σ_1 , and normal to σ_3 , and shear fractures form parallel to σ_2 as a conjugate set, c. 30 degrees either side of σ_1 (Belayneh, 2004).

The conjugate shear fracture systems can be separated from other sets of fractures as follows: the conjugate fracture sets are determined by using criteria such as intersection of the fractures, mutually, opposite sense of displacement, constancy of the angle between them under a general change of their orientation, analogous distribution and connection with regional structures (Twiss and Moores, 1992). The used method is primarily based on the fundamentals of rock mechanics, which suggest that two possible orientations of conjugate shear fractures can develop under the influence of a homogeneous stress field.

Table 1: Stress tensor results in the study area. n: number of data used in the subset; nt: total number of measured data; σ_1 , σ_2 and σ_3 : are the principal stress axes; R: stress ratio; R': stress regime index; QRw is the world stress map quality rank and QRT is the tensor quality rank ranging from A: very good, E: very poor; SHmax: horizontal maximum compressional axes; regime (SS: strike- slip regime and NF: normal regime); and misfit angle using function F5.

Station / Tensor	n/nt	σ_1	σ_2	σ_3	R	Misfit	F5	R	QRw	QRT	SHmax / Shmin	Regime
A3	11/15	16/155	65/284	18/059	0.69	2.8	0.5	1.31	C	C	151	SS
A4a	16/24	01/147	89/312	00/057	0.5	3.6	1.3	1.5	C	C	147	SS
A4b	7/7	70/109	01/201	20/291	0.43	2	1.2	0.43	D	E	021	NF
H1a	17/23	18/147	68/288	13/052	0.65	11.8	5.4	1.35	C	D	144	SS
H1b	10/16	87/188	02/328	02/058	0.22	2	0.3	0.22	C	D	148	NF
J2	13/15	55/186	27/324	20/065	0.88	9.4	8.6	0.88	C	C	144	NF
M1	8/13	73/292	00/201	17/111	0.23	1	0.3	0.23	D	E	020	NF
M2a	17/25	15/136	73/340	07/228	0.64	6.8	2.9	1.36	C	C	137	SS
M2b	10/14	87/200	00/105	03/015	0.04	1.2	0.1	0.04	C	D	105	NF

Accordingly, the principal stress axes can be inferred as: (1) the line of intersection of the conjugate faults is the intermediate stress axis (σ_2); (2) the compressional stress axis (σ_1) bisects the acute angle between the fault planes; and (3) the tensional stress axis (σ_3) bisects the obtuse angle (Price and Cosgrove, 1990; Hancock, 1991; Twiss and Moores, 1992; Lunina et. al., 2005) (Fig. 3a, b). Therefore, the direction of σ_1 was deduced from the conjugate shear fractures in which bisector of the acute angle is parallel to σ_1 , and from the extensional fractures that form parallel to σ_1 (Fig.3c).

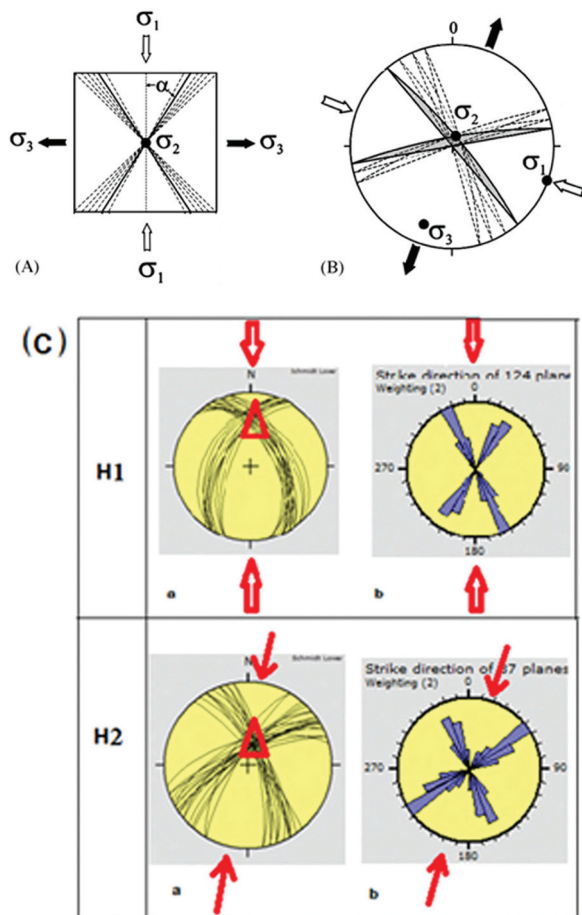


Figure 3. The concept of statistical analysis for the determination of the conjugate fracture systems and reconstruction of the principal stress directions: (A) scheme of the scattering development, α , angle of shear (after Lunina et. al., 2005); (B) diagram of the principal stress directions (σ_1 , σ_2 and σ_3 are the maximum, intermediate and minimum compressive stress axes, respectively (after Lunina et. al., 2005)) obtained from a set of conjugate fractures; (C) examples from the study area in stations H1 and H2 (equal-area lower hemisphere projection (left), and rose diagrams (right); red arrows indicate σ_1 , triangle represents σ_2).

4.2. Method (stress inversion)

Most of the inversion methods of obtaining stress tensor from fault-slip data are based on Wallace (1951) and Bott (1959) hypotheses that assume slip occurs parallel to the direction of the maximum shear stress on fault plane.

The fault-slip data are inverted to obtain the parameters of the reduced stress tensor. These parameters are the principal stress axes σ_1 , σ_2 and σ_3 , where $\sigma_1 > \sigma_2 > \sigma_3$ and the ratio of principal stress differences $R = (\sigma_2 - \sigma_3) / (\sigma_1 - \sigma_3)$, which defines the shape of the stress ellipsoid (Delvaux et. al., 1997).

According to Delvaux et. al. (1997), the stress regime is a function of the orientation of the principal stress axes and the shape of the stress ellipsoid (R): extensional when σ_1 is vertical, strike-slip when σ_2 is vertical, and compressional when σ_3 is vertical. Therefore, they introduced the stress regime index R' . The relations between R and R' are:

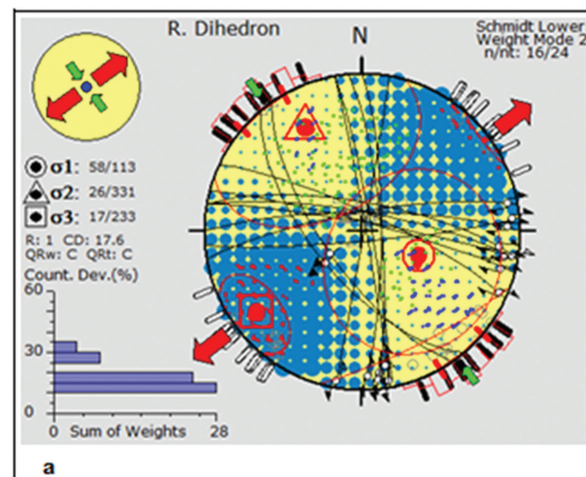
$R' = R$ when σ_1 is vertical (extensional stress regime)

$R' = 2 - R$ when σ_2 is vertical (strike-slip regime)

$R' = 2 + R$ when σ_3 is vertical (compressional regime)

R' defines the stress regime on a continuous scale from 0 (radial extension) to 3 (radial compression), in detail from 0 to 1 for normal faulting regime (σ_1 sub-vertical), from 1 to 2 for strike-slip regime (σ_2 sub-vertical), and from 2 to 3 for thrust faulting regimes (σ_3 sub-vertical).

The data were processed interactively by the Win TENSOR program; first using the "Right Dihedron method" a graphical method for determining the possible orientations of σ_1 and σ_3 (Angelier and Mechler, 1977). The initial result is used as a starting point for the iterative grid-search "Rotational Optimization" procedure using the misfit function F_5 in the Win TENSOR program package (described as F_3 in Delvaux and Sperner, 2003; Delvaux, 2012) (Fig. 4).



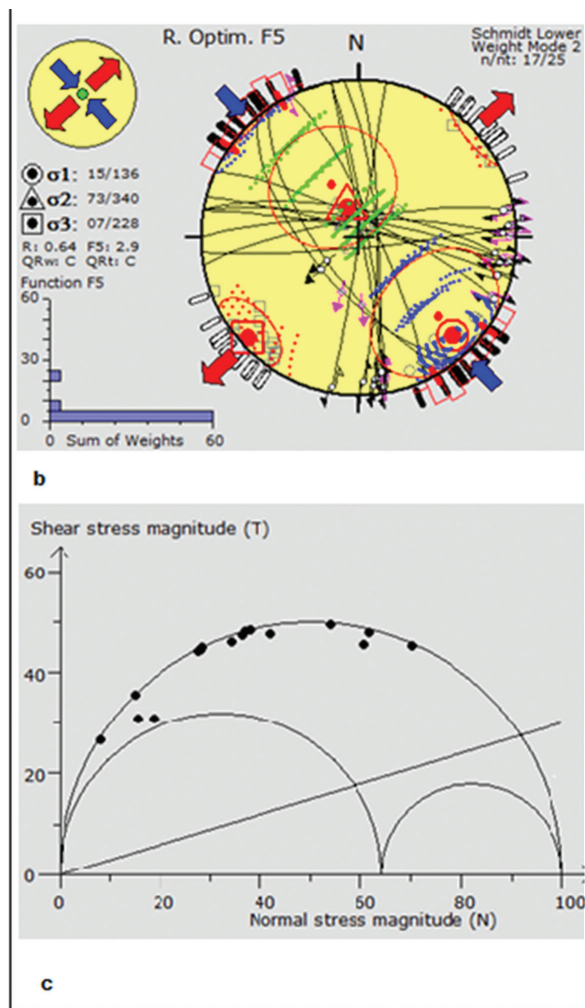


Figure 4. Example of tensor solutions in the study area: a) Right Dihedron method, green arrows for maximum principal compression, red arrows for minimum principal compression, the histogram gives the counting deviation angles; b) Rotational Optimization, blue arrows for maximum principal compression, red arrows for minimum principal compression, the histogram gives the distribution of measured data against the function F5. For best fit F5 approaches 0 for all measurements (for more details see Table 1); c) Mohr diagram illustrates the stress regime and the area of fault activation (the failure curve is based on Byerlee, 1978 initial friction angle 16.7).

5. Results

5.1. Folds

The Ibbin-Housha fold belt that is described by Atallah and Mikbel (1992) (Fig. 1) is a well-developed fold belt, consisting of anticlines and synclines with sub-parallel axes trending mainly ENE- WSW to NE- SW(Fig. 2) .

In the study area, the NE extremity of the Ibbin-Housha fold belt to the northeast of Housha is marked by a single anticline that plunges to the NE (Fig. 2). This anticline was investigated locally in the present study (M2). Its ENE-WSW oriented axis (Fig. 5) indicates NNW-SSE directed local compression. Because the anticline was formed in Umm Rijam Formation (Eocene), the related stress is attributed to Post-Eocene tectonic regimes.

The anticline is cross cut by several E-W high-angle normal faults (Figs. 6c and d). In addition, oblique and horizontal slickenlines were observed on some fracture planes

along this anticline (Fig. 6e). In the northwestern part of the study area, two anticlines with sub-parallel axes trending NE-SW were also delineated in the present study (Fig. 2).

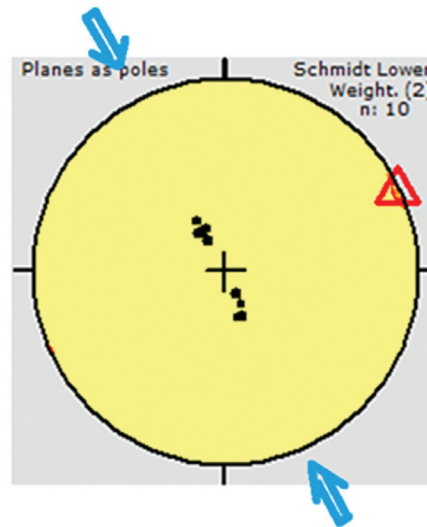


Figure 5. Example of ENE slightly plunging anticline in station M2; solid black dots are the poles to bedding and the triangle is the hinge orientation, the blue arrows indicate the direction of compression .

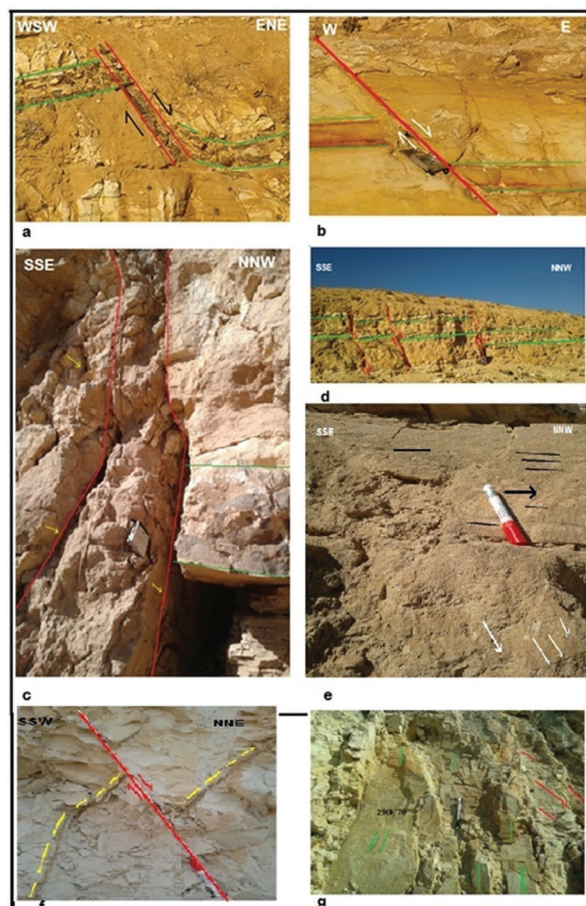


Figure 6. Field examples of normal and oblique-slip faults. a: normal fault zone filled chert (silicification) in station- A4. b: low-angle-normal fault in station- A5. c: oblique-slip fault (yellow arrows indicate slickensides show normal- sinistral slip) cut fold limb in station-M2. d: vertical to high-angle normal faults cut fold limb at station- M2. e: superposition of oblique and horizontal slickensides in station- M2. f: normal fault crosscut vein in station- H1. g: vertical and oblique slickenlines in station- A4.

5.2. Syndepositional structures

Syndepositional structures were observed in Paleocene rocks of Muwaqqar Formation of station-A1 (Fig. 7), in which the throw of the NE-SW oriented low-angle normal fault of marker 1 at the bottom is greater than those of the other markers (Fig.7). In addition, beds, at the top of the fault, appear to be offset less or not at all than beds 1, 2 and 3. Bed 4 may not be disrupted by the fault; however, it is possible that the fault continues toward the top-left of the photo (Fig.7).



Figure 7. A syndepositional fault in Paleocene rocks of station- A1; stereographic projection lower hemisphere of low angle normal fault, the fault strikes NE- SW and dips toward NW, the fault shows decreasing throw upwards (marker 1 has greater throw than other markers 2, 3, and 4).The fault movement occurred during the Paleocene under NW- SE extension.

5.3. Fault- slip data

The mapped faults in the study area are trending NW-SE, N-S, NE-SW and E-W (Fig. 2). Two major strike-slip faults

are seen at the western half of the study area. The first fault extends from Housha in the south to the northern border of the study area in N-S direction. It shows oblique slickensides of normal and sinistral components of slip on its surface that appears along road cut (Fig. 8a). The second fault extends from Mughayer in the southeast in a general NW-SE trend toward station-A2 in northwestern part of the study area; this fault is of dextral-slip (Fig. 2). These two faults could be conjugate, resulting from NNW-SSE compressional stresses.

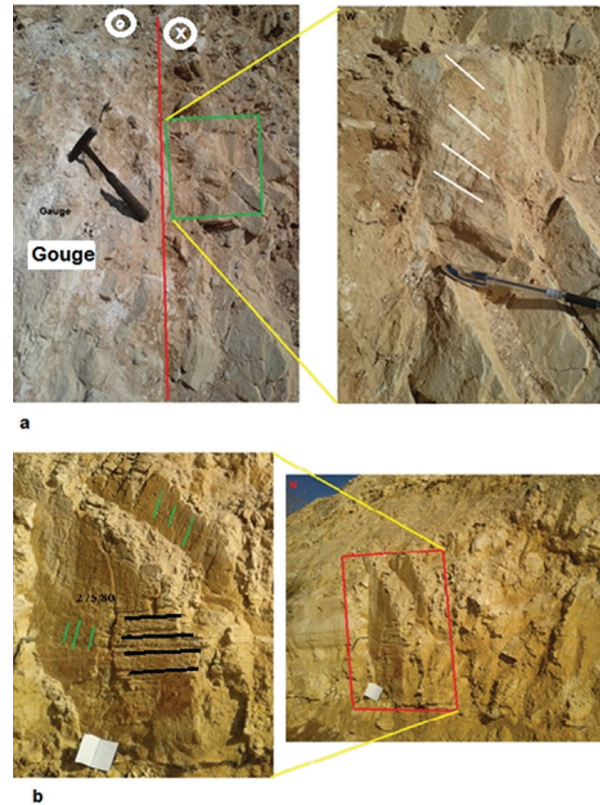


Figure 8. Field examples of fault kinematic indicators. a: Sinistral strike- slip fault (red line), inset photo shows slickenlines on bedding planes of normal- sinistral slip (station- A3). b: superposition of normal slip and strike- slip slickenlines on a fault plane (station- A4).

The number of the measured fault-slip data in the field is 142, but that of those used in defining stress states is 109, that is, the 33 measurements were omitted because they are incompatible with slip deviations and show unreasonable results. This may be due to the measurement error in the field or to local block rotation around fault blocks. Most prominent measured meso-scale faults in the study area are of strike-slip and normal displacement (Fig. 8). All fault slip data were measured in Umm Rijam Formation (Eocene) except for those of station-H1, measured in Muwaqqar Formation (Paleocene).

The results of stress inversion applied on the measured data from different stations (Fig. 9 and Table 1) are as follows:

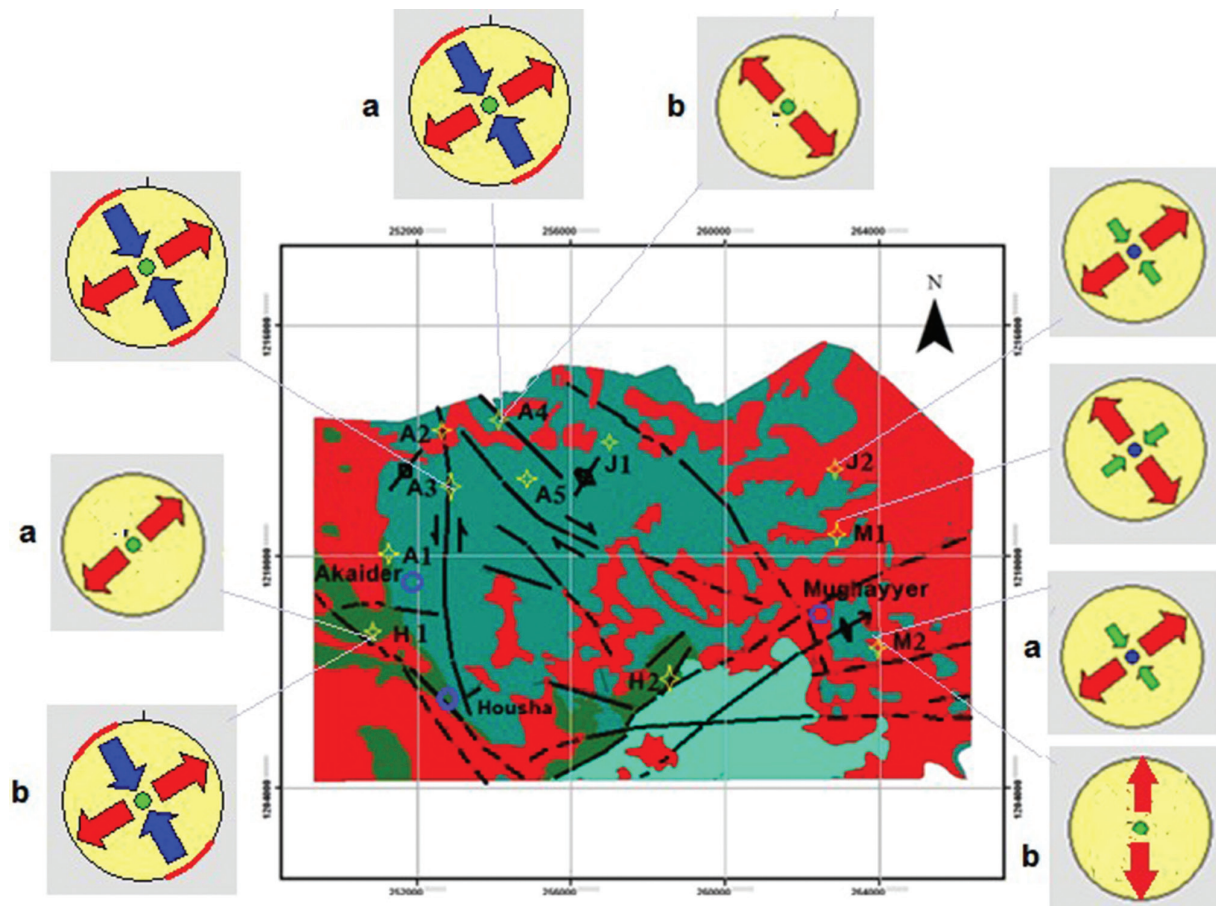


Figure 9. Tensor solutions in the study area. Blue, red and green arrows show the maximum, minimum and intermediate principal compression, respectively.

5.3.1. Station A3

Eleven fault-slip data were measured in a road cut located in the northwestern part of the study area along an N-S sinistral strike-slip fault (Fig. 9 and Table 1). The stress tensor is characterized by σ_1 :16/ 155, σ_2 : 65/ 284, σ_3 :18/ 059 and $R= 0.69$. The determined stress tensor belongs to strike-slip regime and indicates NNW-SSE directed compression and ENE-WSW directed extension. It is responsible for the activation of the measured conjugate N-S sinistral and WNW-ESE dextral strike-slip faults.

5.3.2. Station A4

Twenty-three measurements were measured in a cliff outcrop located in the northern most part of the study area (Fig.9 and Table 1). Two stress tensors were obtained from the whole fault population; the first stress tensor (A4-a) is characterized by σ_1 : 01/ 147, σ_2 : 89/312, and σ_3 : 00/057 with $R= 0.5$. It belongs to strike-slip regime and indicates NNW-SSE oriented compression and ENE-WSW extension direction. It is responsible for the activation of measured conjugate N-S sinistral and WNW-ESE dextral strike-slip faults. The second stress tensor (A4-b) is characterized by σ_1 : 70/ 109, σ_2 : 01/ 201, and σ_3 : 20/ 291 with $R= 0.43$. It belongs to extensional regime and indicates WNW-ESE extension direction. This tensor produced the NNE-SSW normal faults.

5.3.3. Station H1

Twenty-seven fault-slip data were measured in a quarry of Muwaqqar Formation (Paleocene) located in the western part of the study area along an N-S sinistral fault (Fig.9 and Table 1). Two stress tensors were obtained from the whole fault population; the first stress tensor (H1-a) is characterized by σ_1 : 18/147, σ_2 : 68/288, and σ_3 : 13/052 with $R= 0.65$. It belongs to strike-slip regime and indicates NNW-SSE directed compression and ENE-WSW directed extension. It is responsible for the activation of measured N-S sinistral strike-slip faults. The second stress tensor (H1-b) is characterized by σ_1 : 87/ 188, σ_2 : 02/ 328, and σ_3 : 02/ 058 with $R= 0.22$. It belongs to the extensional regime and indicates ENE-WSW extension direction. This tensor produced the NNW-SSE normal faults.

5.3.4. Station J2

Thirteen fault-slip data were measured in a road cut located in northeastern part of the study area (Fig.9 and Table 1). The determined stress tensor is characterized by σ_1 : 55/ 186, σ_2 : 27/ 324, and σ_3 : 20/ 065 with $R= 0.88$. It belongs to extensional regime and indicates ENE-WSW extension direction. This tensor is responsible for the activation of measured NNW-SSE normal faults.

5.3.5. Station M1

Eight fault-slip data were measured in a quarry located in the east central part of the study area (Fig. 9 and Table 1). The stress inversion analysis reveals a stress tensor that is characterized by σ_1 : 73/ 292, σ_2 : 00/ 201, and σ_3 : 17/ 111 with $R= 0.23$. It belongs to the extensional regime and indicates ESE-WNW oriented extension. This tensor is responsible for the activation of the measured NNE to N-S trending normal faults.

5.3.6. Station M2

Twenty-seven fault-slip data were measured in a quarry located in the southeastern part of the study area in an anticline outcrop (Fig. 9 and Table 1). Two stress tensors were obtained from the whole fault population; the first stress tensor (M2-a) is characterized by σ_1 : 15/ 136, σ_2 : 73/ 340, and σ_3 : 07/ 228 with $R= 0.64$. It belongs to strike-slip regime and indicates NW-SE oriented compression and NE-SW oriented extension. It is responsible for the activation of the conjugate N-S sinistral and WNW-ESE dextral strike-slip faults. The second stress tensor (M2-b) is characterized by σ_1 : 87/ 200, σ_2 : 00/ 105, and σ_3 : 03/ 015 with $R= 0.04$. It belongs to the extensional regime and indicates a general N-S to NNE-SSW oriented extension. This tensor is of local extensional direction produced the E-W normal faults that affects the stratigraphic horizons of the bedding planes of the anticline in this station, in which the downthrows along these faults reach up to 90 cm (Fig. 6d).

5. 4. Fractures

According to the information obtained from the investigation of fractures, shown in rose diagrams in Figure (10), it is obvious that different fracture sets were produced in the study area. These fractures can be categorized with respect to their failure mechanism or structural setting as follows:

- 1- Extensional fractures are observed in stations A1 and J1 and their NNW-SSE strikes indicate the direction of σ_1 (Figs.10, A1-a and J1,11a). All fractures have a dip angle greater than 80 degrees.
- 2- Conjugate shear fractures are dominant in stations A5, H1 and H2 and have strikes in various directions, e.g., N-S, NE-SW, NW-SE, NNW-SSE, NNE-SSW and ESE-WNW (Figs. 10, 11 c-e). However, σ_1 deduced from these fractures is different in the stations; therefore, it varies as NNW-SSE in A5, NNE-SSW in H2, and ENE-WSW in H1-b (Fig. 11 c). All fractures related

to these directions have a dip angle greater than 70 degrees. In H1, also, there are quite large numbers of conjugate shear fractures that indicate vertical σ_1 (Figs. 10, H1-a, 11 d). These fractures have dip angles less than 70 degree.

- 3- Shear fractures are observed in stations A1, A2 and A3 (e.g., Fig. 11 f).
- 4- Orthogonal fractures are measured in stations A2 and A4 (Fig. 11 b).

In the case of the last two categories, insufficient kinematic and temporal restrictions posed an impediment to deducing stress direction.

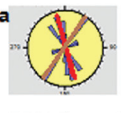
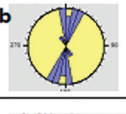
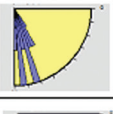
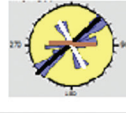
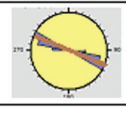
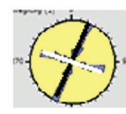
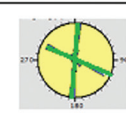
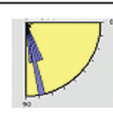
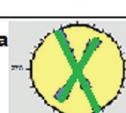
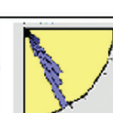
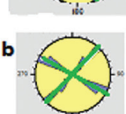
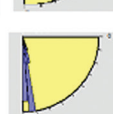
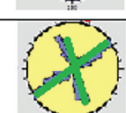
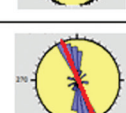
Station	Number of measurements	Strike direction	Dip angle	Fracture type /system	Stress (σ_1)
A1	54			extensional & shear	
	34			normal faults	
A2	63			orthogonal & shear	??
A3	35			shear	
A4	44			orthogonal	??
A5	70			conjugate shear	
H1	124			Conjugate shear	σ_1 vertical
	40			conjugate shear	
H2	37			Conjugate shear	
J1	78			extensional	

Figure 10. Results of 579 fracture data and the deduced σ_1 direction in different stations of the study area. The red, brown, green, and black-and-white lines delineate the strike of extensional, shear, conjugated shear, and orthogonal fractures, respectively.

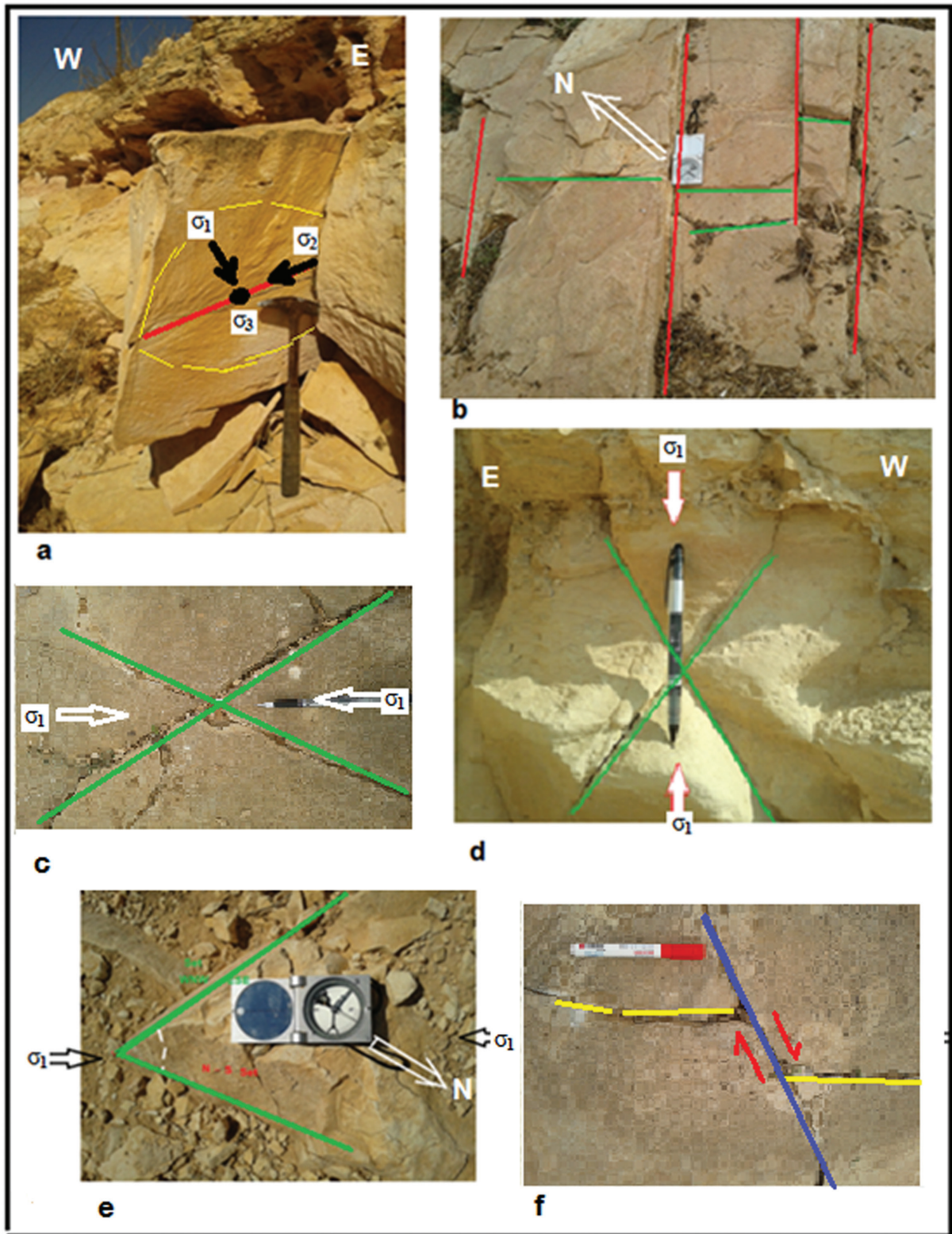


Figure 11. Field examples of some kinematic indicators. a: plumose sub- vertical tension fracture in station- A5 shows the directions of the principal stresses. b: orthogonal joint system (master joints in red color and cross joints in green color) in station A2. c, d and e: conjugate shear fractures in which the acute bisector is parallel to σ_1 (c, d in H1; e in A2) f: right-lateral displacement affects bedding surface in station- A2.

6. Interpretation of results

The results of stress inversion on fault-slip data collected in six sites reveal the existence of strike-slip and extensional regimes. In this regard, the obtained results show that σ_1 (SHmax) and σ_3 (Shmin) are generally sub-horizontal and σ_2 is sub-vertical in four stress tensors (e.g., A3, A4-a, H1-a, and M2-a), and their R' value range between 1.31- 1.50. Therefore, they belong to a major strike-slip regime in which σ_1 swings around NNW-SSE (N137°E - N151°E) (Table 1 and Figs. 9, 12). On the other hand, in five stress tensors (A4-b, H1-b, J2, M1 and M2-b) σ_1 is vertical and σ_2 (SHmax) and σ_3 (Shmin) are (sub) horizontal (Table 1 and Figs. 9, 12), and their R' values vary between 0.04- 0.88. Although these parameters indicate an extensional regime, the direction of maximum extension (σ_3) differs as 1- NNE-SSW (N 015°E - N111°E) in A4-b and M2-b, 2- ENE-WSW in H1-b and J2, and 3- WNW-ESE in M1. The first two stress states are consistent with the Neogene main extension determined by previous works (e.g., Diabat et al., 2004; Hardy et al., 2010). The third stress state probably is related to late extensional activities in Miocene to Pleistocene, as a similar stress state is recognized by Hardy et al., (2010) in Galilee area (north Palestine).

According to field observations (e.g., in A4, H1 and M2) many fault planes show at least two phases of superimposed movements. Kinematic indicators (Figs. 6 and 8) show that the movements with normal sense are overprinted on those with strike-slip sense. This implies that the extensional stress regime is younger than the strike-slip regime in the study area.

According to the direction of σ_1 resulted from extensional and conjugate shear fractures, in some stations (A1-a, A5 and J1) the direction is NNW-SSE. This trend is in a good accordance with the NNW-SSE compression direction resulted from fault slip analysis.

In general, the direction of maximum compression (NNW-SSE), resulting from the analysis of both fault-slip data and extensional as well as conjugate shear fractures, is in agreement with NNW-SSE direction resulted from fold measurements of the present study – also the general trend of folds in a larger scale in Jordan. In addition, it is compatible with the results of other works in the region and along DST fault in which the relative stresses are considered active since the Middle Miocene (e.g., Eyal and Reches, 1983; Badawy and Horváth, 1999; Hardy et al., 2010).

Since the chronostratigraphy in the study area was based on the relative vertical positions of lithologic units, similar lithology, in sites in which data are collected, does not allow a temporal constraining of recognized stress states more precisely. Detailed dating of lithologic units in the study area, in the future, may help to put more strict restriction, in terms of temporal variation of defined stress states.

On the whole, in the present study, through the analysis of fault-slip data in Badia, Northwestern of Jordan, two main stress regimes are recognized: 1- a strike slip regime with NNW-SSE direction of σ_1 . This regime is responsible for the activation of WNW-ESE to E-W dextral and N-S sinistral faults; 2- an extensional regime (normal fault setting) with three different direction of σ_3 , i.e., NNE-SSW, ENE-WSW and WNW-ESE. The existence of these regimes is supported by other geologic evidence such as syn-depositional normal faults, extensional and conjugate shear fractures. Superposition of movements with a normal sense on those with strike-slip sense suggest young (Neogene) extensional activities in the area; however, these extensional activities are probably local, considering the domination of strike-slip stress regime in larger scale.

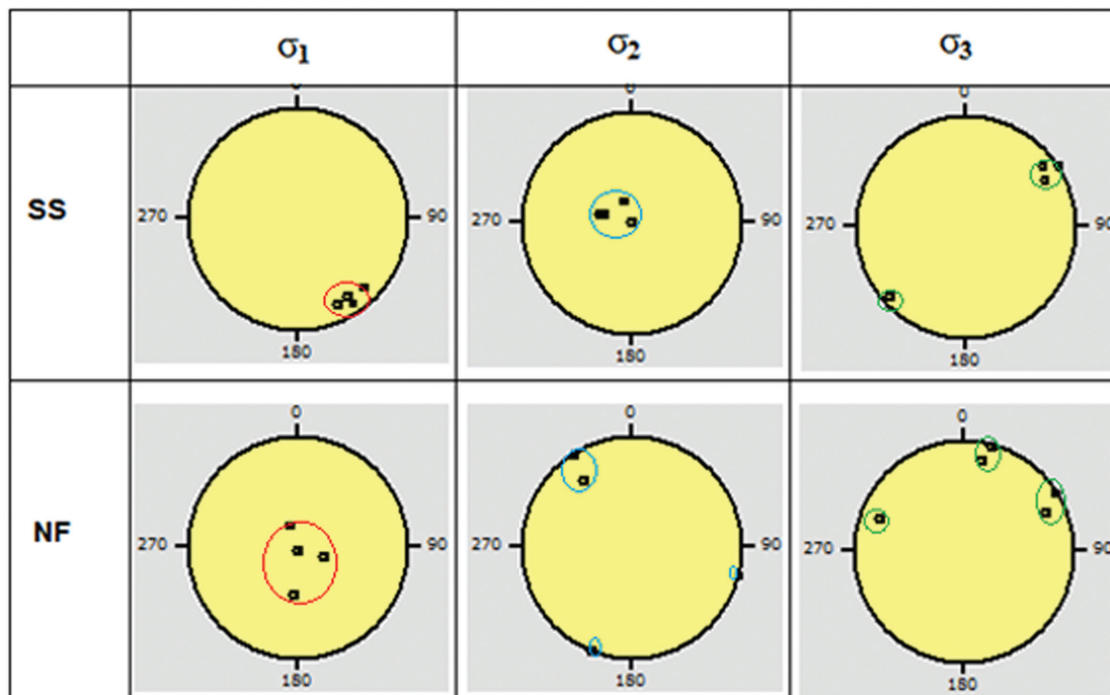


Figure 12. Stress regimes in the study area; SS is strike-slip regime, NF is extensional or normal-slip regime: clusters are the orientation of the principal stress axes; red circle for σ_1 , blue for σ_2 and green for σ_3 .

Acknowledgement

The author is very grateful to Al al-Bayt University as this research was accomplished during the sabbatical year granted. The author also thanks two anonymous reviewers for their constructive comments, which substantially improved the quality of the manuscript.

References

- [1] Angelier, J., 1989. From orientation to magnitudes in palaeostress determinations using fault slip data. *J. Struct. Geol.*, 11: 37-50.
- [2] Angelier, J., 1994. Fault-slip analysis and paleostress reconstruction. In: *Continental Deformation* (ed. Hancock, P.L.), 1 edn., pp. 53- 100. Pergamon Press, U.K., Bristol.
- [3] Angelier, J., and Mechler, P., 1977. Sur une méthode graphique de recherche des contraintes principales également utilisable en tectonique et en séismologie: la méthode de dièdres droites. *Bull. Soc. Geol. Fr.* 7:1309-1318.
- [4] Atallah, M., 1992. On the structural pattern of the Dead Sea Transform and its related structures in Jordan. *Abhath Al-Yarmouk (Pure Sciences and Engineering)* 1, 127-143.
- [5] Atallah, M., Mikbel, Sh., 1992. Structural analysis of the folds between Wadi el- Yabis and the basalt Plateau, northern Jordan. *Dirasat (pure and applied sciences)* 19, 43- 58.
- [6] Badawy, A., Horvath, F., 1999. Recent stress field of the Sinai subplate region. *Tectonophysics* 304, 385- 403.
- [7] Belayneh, M., 2004. Paleostress orientation inferred from surface morphology of joints on the southern margin of Bristol Cannel Basin, UK. In: *Cosgrove, J.W. & Engelder, T. (eds) The initiation, propagation, and Arrest of joints and other fractures.* Geological Society, London, Special Publications 231, 241-255.
- [8] Bell, F. G., 1993. *Engineering Geology.* Black Well Publications London. 359P.
- [9] Bender, F., 1968. *Geology of Jordan.* Borntraeger, Berlin. 196p.
- [10] Bender, F., 1974. *Geology of Jordan;* Berlin, Gebruder Borntraeger.
- [11] Bott, M. H. P., 1959. The mechanics of oblique-slip faulting. *Geological Magazine* 96, 109- 117.
- [12] Burdon, D. J., 1959. *Handbook of the Geology of Jordan: to accompany and explain the three sheets of 1: 250,000 Geological Map, East of the Rift.*
- [13] Byerlee, J.D, 1978: Friction of rocks. *Pure and Applied Geophysics.* 116: 615-626.
- [14] Delvaux, D., 2012. Release of program Win-Tensor 4.0 for tectonic stress inversion: statistical expression of stress parameters. *EGU General Assembly, Vienna, 2012.* *Geophysical Research Abstracts*, Vol. 14, EGU 2012- 5899. Program available at [http:// users.skynet.be/ damien.delvaux/ Tensor/ tensor- index.html](http://users.skynet.be/damien.delvaux/Tensor/tensor-index.html).
- [15] Delvaux, D., Sperner, B., 2003. Stress tensor inversion from fault kinematic indicators and focal mechanism data: the TENSOR program. *Geological Society of London, Special Publications* 212, 75- 100.
- [16] Delvaux, D., Moëys, R., Stapel, G., Petit, C., Levi, K., Miroshnich, K., Ruzhich, V., Sankov, V., 1997. Paleostress reconstructions and geodynamics of the Baikal region, Central Asia, Part 2. Cenozoic rifting. *Tectonophysics*, 282, 1- 38.
- [17] Diabat, A., 1999. Paleostress and strain analysis of the Cretaceous Rocks in the Eastern Margin of the Dead Sea Transform, Jordan. Ph.D. thesis, Baghdad University.
- [18] Diabat, A., 2002. Strain analysis of the Cretaceous rocks in the Eastern margin of the Dead Sea Transform, Jordan. *Dirasat* 29, 159-172.
- [19] Diabat, A. (2009). Structural and stress analysis based on fault-slip data in the Amman area, Jordan. *Journal of African Earth Sciences* 54, 155-162.
- [20] Diabat, A., 2013. Fracture systems of granites and Quaternary deposits of the area east of Aqaba: indicators of reactivation and neotectonic activity. *Arabian Journal of Geosciences*, vol. 6, No. 3: 679- 695.
- [21] Diabat, A., Salih, M., and Atallah, M., 2003. Magnitudes of the paleostresses at the Eastern Rim of the Dead Sea Transform Fault, Jordan. *Dirasat*, 30, 1-18.
- [22] Diabat, A., Atallah, M., Salih, M., 2004. Paleostress analysis of the Cretaceous rocks in the eastern margin of the Dead Sea transform. *Journal of African Earth Sciences* 38, 449-460.
- [23] Diabat, A., and Masri, A., 2005. Orientation of the principal stresses along Zerqa- Ma'in Fault, Mu'ta Lil-Buhuth wad-Dirasat. 20: 57- 71.
- [24] Dunne, W.M., Hancock, P.L., 1994. Paleostress analysis of small-scale brittle structures. In: Hancock, P.L. (Ed.) *Continental Deformation.* Pergamon, Oxford, 101- 120.
- [25] Eyal, Y., 1996. Stress field fluctuations along the Dead-Sea Rift since the middle Miocene. *Tectonics* 15: 157-170.
- [26] Eyal, y., and Reches, Z., 1983. Tectonic analysis of the Dead Sea Rift region since the late Cretaceous based on mesostructures. *Tectonics*, 2: 167-185.
- [27] Eyal, M., Eyal, Y., Bartov, Y., Steinitz, G., 1981. Tectonic development of the western margin of the Gulf of Elat(Aqaba) rift. *Tectonophysics* 80, 39-66.
- [28] Eyal, Y., Gross, M.R., Engelder, T., Becker, A., 2001. Joint development during fluctuation of the regional stress field in southern Israel. *Journal of Structural Geology*, 23: 279-296.
- [29] Freund, R., Garfunkel, Z., Zak, I., Goldberg, M., Weissbrod, T., Derin, B., 1970. The shear along the Dead Sea rift. *Philosophical Transaction of the Royal Society of London* 267, 107- 130.
- [30] Garfunkel, Z., 1981. Internal structure of the Dead Sea leaky transform (rift) in relation to plate kinematics. *Tectonophysics* 80, 81- 108.
- [31] Goodman, R. E. 1980. *Introduction to rock mechanics.* John Wiley and sons. 478 P.
- [32] Hancock, P.L., 1991. Determining contemporary stress directions from neotectonic joint systems. In: Whitmarsh, R.B., Bott, M.H.P., Fairhead, J.D., Kusnir, N.J., (Eds.), *Tectonic Stress in the Lithosphere.* Phil. Trans. Royal. Soc. London A 337, 29-40.
- [33] Hardy, C., Homberg, C., Eyal, Y., Barrier, E., Muller, c., 2010. Tectonic evolution of the southern Levant Margin since the Mesozoic. *Tectonophysics* 494, 211-225.
- [34] Jensen, E., Cembrano, J., Faulkner, D., Veloso, E., Arancibia, G., 2011. Development of a self-similar strike-slip duplex system in the Atacama Fault system, Chile. *Journal of Structural Geology*, 33, 1611- 1626.
- [35] Kersten, R. W. O., 1990. The Stress Distribution Required for Fault and Joint Development. *Proceedings of the International Conference of Mechanics of Jointed and Faulted Rock*, Vienna, Austria, H. P. Rossmanith (ed.), Blakema, Rotterdam, 251 P.
- [36] Leeder, M.R., Gawthorpe, R.L., 1987. Sedimentary models for extensional tilt-block/half graben basins. In: Coward, M.P., Dewey, J.F., Hancock, P.L. (Eds.), *The Geological Society Special Publication* 28, 139-152.
- [37] Lumina, O. V., Mart, Y., Gladkov, A. S., 2005. Fracturing patterns, stress fields and earthquakes in the Southern Dead Sea rift. *Journal of Geodynamics* 40 , 216-234.
- [38] Mikbel, Sh., 1986. Some relevant tectonical and geotechnical considerations of south Amman area/ Jordan.. *Dirasat* 7, 215-225.
- [39] Mikbel, Sh., Zacher, W., 1981. The WadiShueib structure in Jordan. *Neues Jahrbuch fuer Geologie und Paleontologie Monatshefte* 9, 571-576.
- [40] Pollard, D.D. and Aydin, A., 1988: progress in understanding jointing during the past century. *Geological Society of America Bulletin*, 100, 1981-1204.
- [41] Powell, J. H., 1989. Stratigraphy and sedimentation of the phanerozoic rocks in central and south Jordan. *Geological mapping division, natural resources authority, Jordan. Bulletin* 11, 130p.

- [42] Price, N.J., Cosgrove, J.W., 1990. Analysis of Geological Structures. Cambridge University Press.
- [43] Price, N.J., 1966, Fault and joint development in brittle and semi-brittle rocks. Pergamon press, Oxford, 176 pp.
- [44] Quennell, A., 1958. The structure and evolution of the Dead Sea rift. *Quaternary Journal of the Geological Society*, 64: 1- 24.
- [45] Quennell, A.M., 1983. Evolution of the Dead Sea Rift. A review, First Jordanian Geologic Conference 460-482.
- [46] Salameh, E., Zacher, W., 1982. Horizontal stylolites in Jordan. *Neues Jahrbuch fuer Geologie und Paleontologie Monatshefte* 8, 504- 512.
- [47] Sassi, W., Faure, J. L., 1996. Role of faults and layer interfaces on the spatial variations of stress regime in basins: inferences from numerical modeling. In: Cloetingh, S., Ben-Avraham, Z., Sassi, W., Horvath, F. (Eds.), *Dynamics of Basin Formation and strike-slip Tectonics*, Tectonophysics, 266, 101- 119.
- [48] Tripathy, V., Saha, D., 2013. Plate margin paleostress variations and intercontinental deformations in the evolution of the Cuddapah basin through Proterozoic. *Precambrian Research*, 235, 107- 130.
- [49] Twiss, R.J., Moores, E.M., 1992. *Structural Geology*. W.N. Freeman and Company Press, New York.
- [50] Wallace, R. E., 1951. Geometry of shearing stress and relation to faulting. *Journal of Geology* 59, 118-130.
- [51] Zain Eldeen, U., Delvaux, D., Jacobs, P., 2002. Tectonic evolution in the Wadi Araba Segment of the Dead Sea Rift, Southwest Jordan. EGU Stephan Mueller Special Publication Series 2, 63- 81.